Available at
www.ElsevierMathematics.com
POWERED BY SCIENCE DIRECT®

Applied Mathematical Modelling 28 (2004) 241–254

APPLIED MATHEMATICAL MODELLING

www.elsevier.com/locate/apm

Comparison of three buoyancy extended versions of the k–ϵ–$\overline{t'^2}$ model in predicting turbulent plane plume

Anupam Dewan *, Kalyan Kalita, Anoop K. Dass

Department of Mechanical Engineering, Indian Institute of Technology Guwahati, Guwahati 781039, India

Received 5 June 2002; received in revised form 8 May 2003; accepted 10 June 2003

Abstract

In the present paper, turbulent plane plume in a quiescent ambience has been numerically studied using three different versions of the buoyancy extended k–ϵ–$\overline{t'^2}$ model. The performance of models is analysed by means of a detailed comparison between the predictions and the experimental observations reported in the literature. In addition, the predictions by the Reynolds stress and the heat flux transport (RSHFT) model reported in the literature are also included in the comparison to examine the effectiveness of k–ϵ–$\overline{t'^2}$ models relative to the higher order RSHFT model. The comparison shows that the mean flow quantities predicted by all the models agree well with the experimental observations. However, considerable differences are observed in the predicted turbulent quantities.

Keywords: Plane plume; Turbulence models; Heat flux; Buoyancy production

1. Introduction

The standard k–ϵ model [1] is widely used but is not capable of properly capturing the effect of buoyancy in a flow and as a remedy it has been extended by Lumley [2] and Launder [3]. Hossain and Rodi [4] reviewed these model proposals. Gibson and Launder [5] extended Launder's model [3] to predict horizontal surface jet and mixing layer. Chen and Rodi [6] proposed k–ϵ–$\overline{t'^2}$ model based on Launder's model [3] and used it to predict the far field behaviour of vertical buoyant jets. Chen and Chen [7] used the model of Chen and Rodi [6] to predict the centreline mean and turbulent quantities of plane and axisymmetric buoyant jets from the exit to the self-similar region

* Corresponding author. Tel.: +91-361-2690321 to 2690328; fax: +91-361-2690762.
E-mail address: adewan@iitg.ernet.in (A. Dewan).

0307-904X/$ - see front matter
doi:10.1016/S0307-904X(03)00138-0

Nomenclature

c's	model constants
G_k	production of k due to buoyancy
g	acceleration due to gravity
k	turbulent kinetic energy
P_k	production of k by shear stress
P_t	production of temperature fluctuations
Pr_t	turbulent Prandtl number
T	mean temperature
ΔT	$= T - T_\infty$
$\overline{t'^2}$	mean square temperature fluctuations
u	mean velocity along streamwise (x) direction
v	mean velocity along cross-stream (y) direction
$\overline{u'v'}$	Reynolds shear stress
$\overline{u't'}$	streamwise heat flux
$\overline{v't'}$	cross-stream heat flux
$\overline{u'^2}$	streamwise velocity fluctuations
$\overline{v'^2}$	cross-stream velocity fluctuations
x	streamwise coordinate
y	cross-stream coordinate
β	coefficient of volumetric expansion
δ_u	velocity halfwidth
δ_t	temperature halfwidth
ϵ	rate of dissipation of k
ϵ_t	rate of dissipation of temperature fluctuations
γ	intermittency factor
Γ	intermittency interaction invariant
ν_t	eddy viscosity
σ_u	normalised centreline velocity $= u_0/B^{1/3}$

Subscripts

∞	ambient temperature
m	maximum value
0	centreline value

for different values of Froude number. Malin [8] proposed another k–ϵ–$\overline{t'^2}$ model to predict plane and axisymmetric jets and plumes. Sini and Dekeyser [9] proposed another buoyancy extended k–ϵ model and predicted the dynamical and thermal fields in plane turbulent jets and forced plume. Bergstrom et al. [10] predicted plane vertical plume using k–ϵ–$\overline{t'^2}$ model where Reynolds stresses and heat fluxes are modelled by nonequilibrium algebraic stress model. In these predictions [9,10] governing flow equations are solved elliptically. Pantokratoras [11] numerically studied the effect of ambient temperature on vertical round and plane turbulent buoyant water jets using k–ϵ–$\overline{t'^2}$ model [7]. However, he used an algebraic relation to correlate water density with temperature on the bases of the equation of state for seawater [11].

Malin and Younis [12] predicted plane and axisymmetric plumes using Reynolds stress and turbulent heat flux transport (RSHFT) model, which is considered as a higher order model compared to the k–ϵ based models.

In the present paper predictions of the self-similar turbulent plane plume in a quiescent ambience are presented using three different versions of buoyancy extended k–ϵ model which include (i) k–ϵ–$\overline{t'^2}$ model proposed by Chen and Rodi [6] (denoted here as model-1), (ii) k–ϵ–$\overline{t'^2}$ model proposed by Malin [8] (model-2) and (iii) model proposed by Kalita et al. [13] (model-3). The predictions are compared with the experimental observations of Ramaprian and Chandrasekhara [14,15]. In addition, the previous predictions obtained by the more complex RSHFT model [12] are also incorporated to compare the performance of this higher order model with that of the buoyancy extended versions of the k–ϵ–$\overline{t'^2}$ model.

The present paper has been arranged in five sections. In Section 2 the governing equations and the features of the different versions of the k–ϵ–$\overline{t'^2}$ model under consideration are described. In Section 3, the boundary conditions applied to the flow configuration and the numerical method adopted for the solution of the governing equations are described. The assessment of the models is presented in Section 4 and concluding remarks are made in Section 5.

2. Governing equations and turbulence models

2.1. Mean flow equations

The flow is assumed to be steady in mean and incompressible and the Boussinesq approximation is applied. The boundary layer forms of the Reynolds-averaged governing equations for the mean velocity and temperature distribution for the turbulent plane plume are then given by

Continuity:

$$\frac{\partial u}{\partial x} + \frac{\partial v}{\partial y} = 0. \tag{1}$$

Streamwise momentum:

$$u\frac{\partial u}{\partial x} + v\frac{\partial u}{\partial y} = \frac{\partial}{\partial y}(-\overline{u'v'}) + g\beta(T - T_\infty). \tag{2}$$

Mean temperature distribution:

$$u\frac{\partial T}{\partial x} + v\frac{\partial T}{\partial y} = \frac{\partial}{\partial y}(-\overline{v't'}). \tag{3}$$

Here u is the mean velocity along the streamwise (x) direction and v is the mean velocity along the cross-stream (y) direction. T and T_∞ are the mean temperature and ambient temperature, respectively. The primed quantities represent fluctuations.

2.2. Turbulence models under consideration

In all the three buoyancy extended versions of the k–ϵ–$\overline{t'^2}$ model considered for the present predictions, the same mean flow equations (Eqs. (1)–(3)) and the modelled transport equation for k, ϵ and $\overline{t'^2}$ are used (Eqs. (12)–(14), respectively) where k denotes turbulent kinetic energy, ϵ denotes rate of dissipation of turbulent kinetic energy and $\overline{t'^2}$ denotes mean square temperature fluctuations. The differences among the three models are in the modelled relations used for the Reynolds shear stress ($\overline{u'v'}$) and turbulent heat fluxes ($\overline{v't'}$ and $\overline{u't'}$) only, which are described here. The main features of the these models are summarised in Table 1.

(i) *Model-1* (Chen and Rodi's model [6]): In this model the modelled relations for the Reynolds shear stress and heat fluxes are derived by simplifying the modelled transport equations for individual stresses and heat fluxes and this is termed as algebraic stress model (ASM) [16]. The simplified relations for the present flow configuration are given below.

Reynolds stress:

$$-\overline{u'v'} = \frac{1-c_0}{c_1}\frac{\overline{v'^2}}{k}\left(1+\frac{kg\beta\frac{\partial T}{\partial y}}{c_h\epsilon\frac{\partial u}{\partial y}}\right)\frac{k^2}{\epsilon}\frac{\partial u}{\partial y}, \tag{4}$$

where

$$\overline{v'^2} = c_2 k. \tag{5}$$

Cross-stream heat flux:

$$-\overline{v't'} = \frac{\overline{v'^2}}{c_h k}\frac{k^2}{\epsilon}\frac{\partial T}{\partial y}. \tag{6}$$

Streamwise heat flux:

$$\overline{u't'} = \frac{k}{c_h\epsilon}\left[-\overline{u'v'}\frac{\partial T}{\partial y} - \overline{v't'}(1-c_{h1})\frac{\partial u}{\partial y} + g\beta(1-c_{h1})\overline{t'^2}\right]. \tag{7}$$

The value of the model constants are $c_0 = 0.55$, $c_1 = 2.2$, $c_2 = 0.53$, $c_h = 3.2$ and $c_{h1} = 0.5$ [6,7].

(ii) *Model-2* (Malin's model [8]): Here the Reynolds stress is modelled using the ASM (Eqs. 4 and 5). The cross-stream heat flux is modelled by using the concept of eddy viscosity [1] and is given as

Table 1
Features of the models

Model considered	Transport equations	$\overline{u'v'}$ modelled by	$\overline{v't'}$ modelled by	$\overline{u't'}$ modelled by
Model-1	k, ϵ and $\overline{t'^2}$	ASM	ASM	ASM
Model-2	k, ϵ and $\overline{t'^2}$	ASM	$-\frac{\nu_t}{\sigma_t}\frac{\partial T}{\partial y}$	$k_h\sqrt{k\overline{t'^2}}$
Model-3	k, ϵ and $\overline{t'^2}$	ASM	ASM	$-\frac{\nu_t}{Pr_t}\frac{\partial T}{\partial x} + k_h\sqrt{k\overline{t'^2}}$

$$\overline{v't'} = -\frac{\nu_t}{\sigma_t}\frac{\partial T}{\partial y}, \tag{8}$$

where

$$\nu_t = \frac{c_\mu k^2}{\epsilon}, \tag{9}$$

Here ν_t is the eddy viscosity, c_μ (=0.09) is the model constant [1] and σ_t (=0.5) is the turbulent Prandtl number [17]. The axial heat flux is modelled as suggested by Malin and Spalding [17] and is given as

$$\overline{u't'} = k_h\sqrt{k\overline{t'^2}}, \tag{10}$$

Here k_h is a model constant and its value is shown in Table 2.

(iii) *Model-3*: In this model the Reynolds shear stress and cross-stream heat flux are modelled using the ASM (Eqs. (4)–(6)). The axial heat flux is obtained by employing the model proposed by Dewan et al. [18]:

$$\overline{u't'} = -\frac{\nu_t}{Pr_t}\frac{\partial T}{\partial x} + k_h\sqrt{k\overline{t'^2}}, \tag{11}$$

Here Pr_t is the turbulent Prandtl number. For the present flow configuration the first term of the right side is negligible. However, the term has been retained for the mathematical consistency of the model.

2.2.1. Transport equations for turbulent quantities

(i) *Turbulent kinetic energy* (k): The modelled transport equation for turbulent kinetic energy is given as [7]

$$u\frac{\partial k}{\partial x} + v\frac{\partial k}{\partial y} = \frac{\partial}{\partial y}\left[\left(c_k\frac{\overline{v'^2}k}{\epsilon}\right)\frac{\partial k}{\partial y}\right] + P_k + G_k - \epsilon, \tag{12}$$

Here $P_k = -\overline{u'v'}\frac{\partial u}{\partial y}$ and $G_k = g\beta\overline{u't'}$ are the shear production and buoyancy production of turbulent kinetic energy, respectively.

(ii) *Rate of turbulent kinetic energy dissipation* (ϵ): The modelled transport equation for ϵ is given as [7]

$$u\frac{\partial \epsilon}{\partial x} + v\frac{\partial \epsilon}{\partial y} = \frac{\partial}{\partial y}\left[\left(c_\epsilon\frac{\overline{v'^2}k}{\epsilon}\right)\frac{\partial \epsilon}{\partial y}\right] + c_{\epsilon 1}\frac{\epsilon}{k}(P_k + G_k) - c_{\epsilon 2}\frac{\epsilon^2}{k}, \tag{13}$$

Table 2
Values of model constants used in the models

Constants	c_k	c_ϵ	$c_{\epsilon 1}$	$c_{\epsilon 2}$	c_{T1}	k_h	c_T
Model-1 [6]	0.225	0.15	1.43	1.92	1.79	–	0.13
Model-2 [8]	0.225	0.15	1.44	1.92	1.79	0.62	0.13
Model-3	0.225	0.15	1.43	1.92	1.79	0.4	0.13

(iii) *Temperature fluctuations* ($\overline{t'^2}$): The mean-square temperature fluctuation ($\overline{t'^2}$) is computed from the following modelled transport equation [7]

$$u\frac{\partial \overline{t'^2}}{\partial x} + v\frac{\partial \overline{t'^2}}{\partial y} = \frac{\partial}{\partial y}\left[\left(c_T\frac{k^2}{\epsilon}\right)\frac{\partial \overline{t'^2}}{\partial y}\right] + P_t - \epsilon_t. \tag{14}$$

Here P_t and ϵ_t are the production and dissipation rate of temperature fluctuations and given as $P_t = -2\overline{v't'}\frac{\partial T}{\partial y}$, $\epsilon_t = \frac{c_{T1}\epsilon\overline{t'^2}}{k}$.

The values adopted for all the constants of model-1 are the same as used by Chen and Rodi [6] with the exception of c_{T1}. Here, we have adopted $c_{T1} = 1.79$ instead of 1.25 as suggested by Chen and Rodi [6]. It is observed from the literature that the value of c_{T1} varies across the plume from 0.125 to 2.0. Bergstrom et al. [10] have used $c_{T1} = 2.0$. Many workers [12,17,18] have suggested that the value for $c_{T1} = 1.79$ is a better choice and therefore, we have adopted this value for c_{T1} ($= 1.79$) in all the three models (model-1, model-2 and model-3) considered here. The main advantage of using $c_{T1} = 1.79$ is that it enables a easy comparison of the three versions of the k–ϵ–$\overline{t'^2}$ model as the same transport equations (12)–(14) along with the almost same values for model constants (c_k, c_ϵ, $c_{\epsilon 1}$, $c_{\epsilon 2}$, c_T and c_{T1}) are used for all models (Table 2). Thus the difference between the three models is only due to the modelled relations used for Reynolds shear stress, cross-stream heat flux, streamwise heat flux terms and the corresponding model constants only.

3. Boundary conditions and numerical method

3.1. Boundary conditions

The mean flow is assumed to be symmetric about the mid-plane of the plane plume and thus the computations are performed over one half of the plume only and the zero flux boundary conditions for all the variables are specified across the plane of symmetry. At the plume edge all the quantities, viz. u, k, ϵ and $\overline{t'^2}$, are set to zero except the mean temperature T which is set equal to the ambient temperature T_∞. At the discharge of the plume, top hat profiles for all the variables are specified.

3.2. Numerical method and code validation

The governing equations presented in Section 2 have been solved using the finite volume method [19]. For this purpose upwind scheme in the streamwise direction and power law scheme [19] in the cross-stream direction are used, thus converting each governing equation into a set of algebraic equations. The system of algebraic equations is solved using line-by line iteration method which employs tridiagonal matrix algorithm. The governing equations are parabolic in nature and therefore, the numerical solution is obtained by marching in the streamwise direction. The computation is stopped when the self-similarity of the plume is achieved. The self-similarity is assumed to be reached when the changes in the growth rates and centerline values of the mean and turbulent quantities are within 1%.

We have used 100 nonuniform grid-points along the cross-stream direction and a step size of 6% of the local velocity half width (δ_u) along streamwise direction. The grids are clustered near the discharge region of the plume. The grid sensitivity of the results is tested by varying the number of grid-points along the normal direction from 100 to 150 while keeping a fixed step size of 6% of the local velocity half width (δ_u) in the streamwise direction. The sensitivity of the streamwise step size is tested by varying the step size from 2% to 8% in an increment of 2% with fixed 100 nonuniform grid-points in the normal direction. In these tests the variation of the mean and turbulent quantities is found to be within 2%.

Two cases are selected to validate the code, (i) the plane jet using the k–ϵ–γ model of Cho and Chung [20] and the plane plume using the k–ϵ–$\overline{t'^2}$ model as used by Malin [8]. Computations are made with the discharge conditions such that the height nondimensionalised by the Morton length scale [18] is much less than unity for the plane jet and more than 15 for the plane plume. The comparison of the present computations with those by Cho and Chung [20] and Malin [8] enables us to validate the present code. The mean and turbulent quantities for the two cases are found to be within 2% of those predicted by Cho and Chung [20] and Malin [8].

4. Assessment of the models

To assess the performance of the models the predictions are compared with the measured data. Measured data for the self-similar turbulent plumes, up to 1980, has been reviewed by Chen and Rodi [21] and by List [22] up to 1982. Subsequently Ramaprian and Chandrasekhara [14,15,23] carried out experiments on the turbulent plane plume. In the present work the measurements made by Ramaprian and Chandrasekhara [14,15] have been chosen for the comparison as their data is seems to be more reliable than those of earlier experiments.

4.1. Mean flow quantities

Growth rate: The predicted velocity growth rate ($\partial\delta_u/\partial x$) and temperature growth rate ($\partial\delta_t/\partial x$) by the three buoyancy extended versions of the k–ϵ model are shown in Table 3 together with the measured data of Ramaprian and Chandrasekhara [15] and the predictions of Malin and Younis [12] by the RSHFT model. The table shows that the velocity growth rate predicted by all the models agrees well with the experimental observation. However, the temperature growth rate is underpredicted by model-1 by about 9% and by model-3 and RSHFT model by about 15%. Considering the large scatter in temperature measurement (10% as stated by Ramaprian and Chandrasekhara [15]) the predictions are satisfactory.

Table 3
Predicted growth rates compared with measurements

Growth rate	Model-1 [6]	Model-2 [8]	Model-3 [13]	RSHFT [12]	Measured data [15]
Velocity	0.119	0.115	0.111	0.105	0.11
Temperature	0.118	0.133	0.11	0.113	0.13

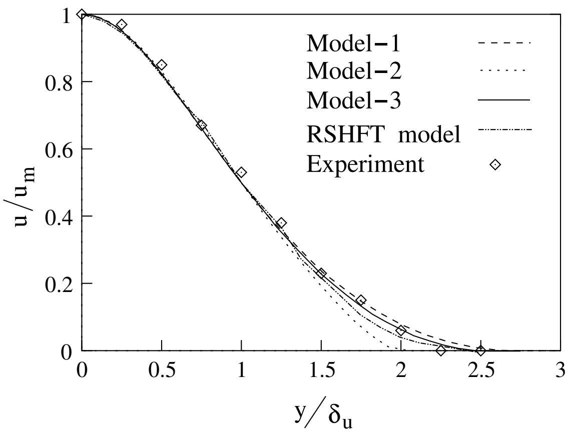

Fig. 1. Comparison of the predictions of the mean velocity by different k–ϵ models with the experimental observations [15] and RSHFT model [12].

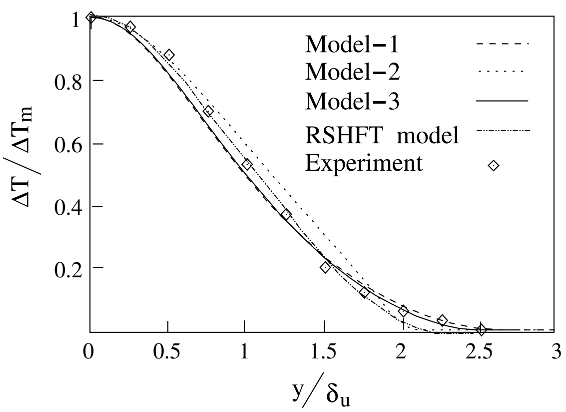

Fig. 2. Comparison of the predictions of the mean temperature profile by different k–ϵ models with the experimental observations [15] and RSHFT model [12].

Mean velocity and mean temperature profiles: The mean velocity and mean temperature profiles predicted by the models under consideration are compared with the experimental observations [15] and the predictions of Malin and Younis [12] by RSHFT model in Figs. 1 and 2, respectively. Both figures show that all the predicted profiles are close to the measured profile except that by model-2.

4.2. Turbulent transport quantities

Reynolds shear stress: Reynolds shear stress ($\overline{u'v'}$) profiles are compared in Fig. 3, which shows that the peak value of Reynolds shear stress predicted by model-3 is higher than the measured value by almost 10%. Considering the experimental uncertainties of 10% [15] the predictions can

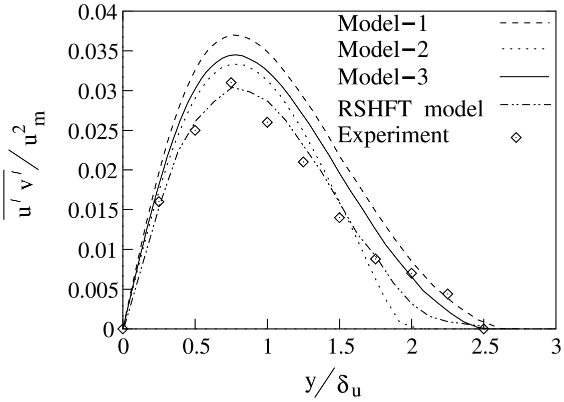

Fig. 3. Comparison of the predictions of the Reynolds shear stress profile by different k–ϵ models with the experimental observations [15] and RSHFT model [12].

be considered as good. The profile shape predicted by model-3 follows the measured profile more closely compared to that by model-1 and model-2. In the three models considered here, the Reynolds shear stress ($\overline{u'v'}$) is modelled by ASM and in RSHFT model a transport equation for $\overline{u'v'}$ is used. The differences in the predicted values of $\overline{u'v'}$ by all the three versions of the k–ϵ are small (maximum deviation is less than 15% of the measured value). The reason for the differences may be the use of different relations for modelling of the heat fluxes ($\overline{u't'}$ and $\overline{v't'}$).

Turbulent cross-stream heat flux: Predicted turbulent cross-stream heat flux profiles are shown in Fig. 4. It is observed that of all the models, the agreement of the prediction by model-3 with the measured data is the best.

Turbulent axial heat flux: In Fig. 5 the predicted profiles of the turbulent axial heat flux are compared with the experimental data. The comparison shows that the agreement between the

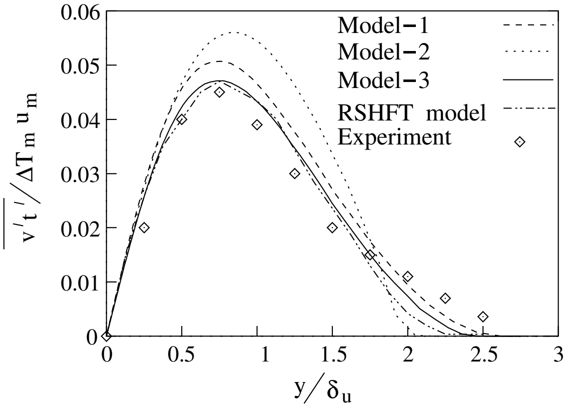

Fig. 4. Comparison of the predicted profiles of the turbulent cross-stream heat flux by different k–ϵ models with the experimental observations [15] and RSHFT model [12].

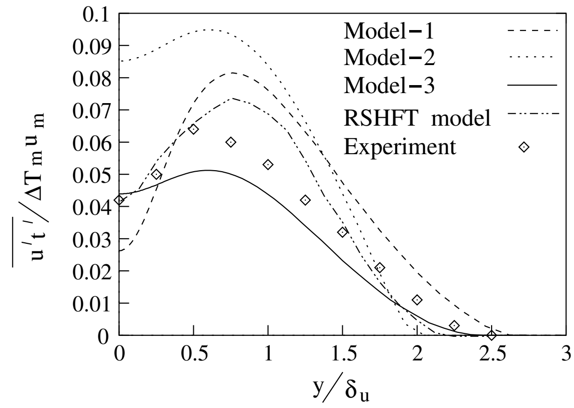

Fig. 5. Comparison of the predicted profiles of the turbulent axial heat flux by different k–ϵ models with the experimental observations [15] and RSHFT model [12].

prediction of model-3 and measurement is satisfactory and superior to the predictions of the other models. Model-2 overpredicts the value of $\overline{u't'}$ near the plane of symmetry by about 105%. This large deviation is probably due to the nonincorporation of the buoyancy effect in computing the cross-stream heat flux and the use of high value for k_h (Malin [8] used $k_h = 0.62$) in model-2. The profile shape predicted by model-1 also deviates from the measured profile. This shows that modelling of $\overline{u't'}$ by ASM [6] and by even more complex transport equation [12] is unable to correctly predict the profile, whereas the simple model used in the model-3 gives better predictions.

Temperature fluctuations: The root mean square (rms) temperature fluctuations profiles predicted by the three different models are shown in Fig. 6. The comparison shows that the predicted profile by model-3 agrees well with the measurement and that by other models show some deviation from measurement.

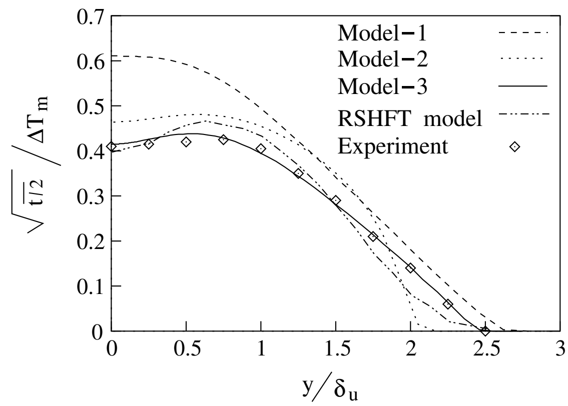

Fig. 6. Comparison of the predicted profiles of the temperature fluctuations by different k–ϵ models with the experimental observations [14] and RSHFT model [12].

4.3. Some aspects of turbulent structure

Predictions of different terms of the turbulent kinetic energy transport equation (12) are compared with the experimental data of Ramaprian and Chandrasekhara [15] in Figs. 7–10. For the dissipation term no experimental data is available and hence no comparison is made. Fig. 7 shows that zero advection at the axis of the plume indicates a constant value of the turbulent kinetic energy along the axis in the self-similar region. This fact, which has been experimentally observed [15], is correctly predicted by all the k–ϵ based models. However, the overall agreement of the advection profile predicted by model-3 is superior to that of other models. Experimental investigation [15] reveals that the influence of buoyancy on diffusion term is insignificant and model-3 is able to predict this trend (Fig. 8). The predicted profile of the production of turbulent

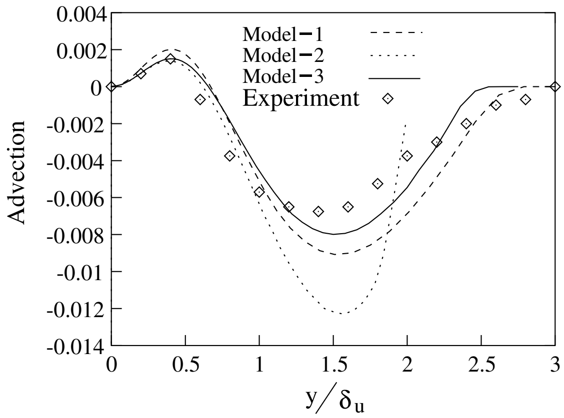

Fig. 7. Comparison of the predicted profiles of the advection term of k equation by different k–ϵ models with the experimental observations [15].

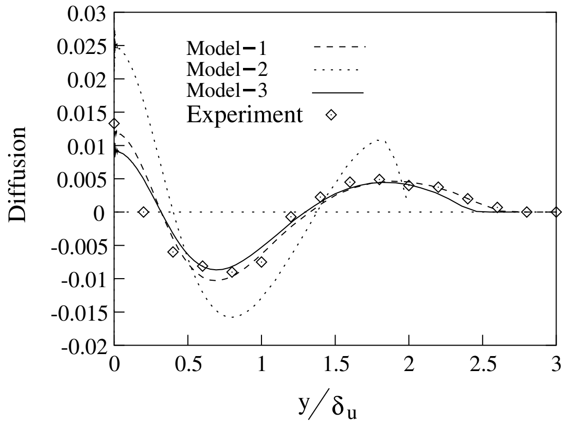

Fig. 8. Comparison of the predicted profiles of the diffusion term of k equation by different k–ϵ models with the experimental observations [15].

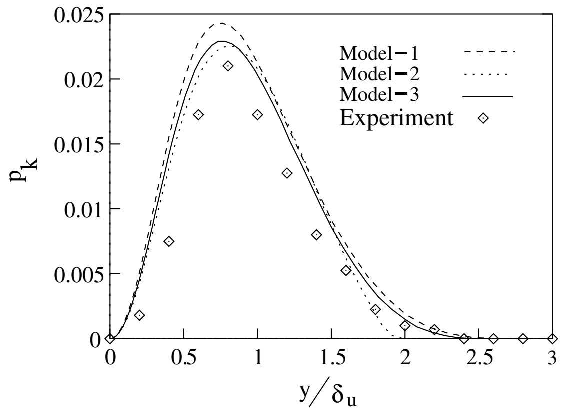

Fig. 9. Comparison of the predicted profiles of the shear production term of k equation by different k–ϵ models with the experimental observations [15].

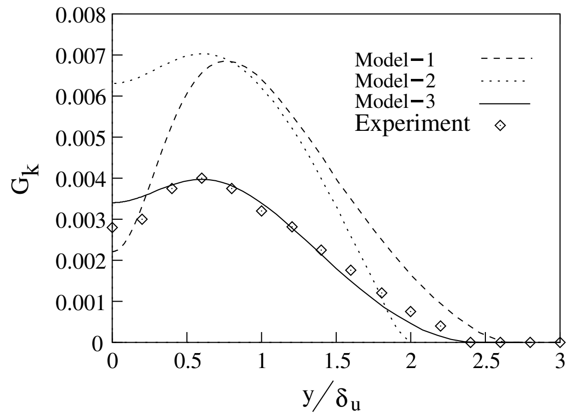

Fig. 10. Comparison of the predicted profiles of the buoyancy production term of k equation by different k–ϵ models with the experimental observation [15].

kinetic energy due to shear (P_k) by the model-3 is closed to the experimental observation (Fig. 9). The direct effect of buoyancy on turbulence is represented by the buoyancy production term G_k. The predicted profiles of G_k are compared with the measurement in Fig. 10. The prediction by model-3 show the best agreement with the measured data [15].

5. Conclusion

From this study it has been observed that the mean quantities of the turbulent plane plume in the self-similar region are predicted accurately by all the models. The predictions of the turbulent quantities, particularly the heat fluxes and temperature fluctuations by the model-3 are superior to the predictions by the earlier used k–ϵ–$\overline{t'^2}$ models. Thus model-3 seems to be the best for this flow configuration. The comparison further reveals that the predictions of most quantities by model-3 and the more complex RSHFT model are almost identical with the exception of axial heat flux and the temperature fluctuations which are better predicted by model-3.

Acknowledgement

The authors thank the referee for invaluable comments, which led to an improvement in the quality of the paper.

References

[1] B.E. Launder, D.B. Spalding, The numerical prediction of turbulent flows, Comput. Methods Appl. Mech. Engrg. 3 (1974) 269–289.
[2] J.L. Lumley, A model for computation of stratified turbulent flow, in: International Symposium on Stratified Flows, Novosibirsk, 1972.
[3] B.E. Launder, Turbulence model and their experimental verification, Technical Report HTS/73/26, Department of Mechanical Engineering, Imperial College, London, UK, 1973.
[4] M.S. Hossain, W. Rodi, Equations for turbulent buoyant flows and their modelling, Technical Report SFB 80/T/46, University of Karlsruhe, Karlsruhe, Germany, 1974.
[5] M.M. Gibson, B.E. Launder, Ground effects on pressure fluctuations in the atmospheric boundary layer, J. Fluid Mech. 86 (1978) 491–506.
[6] C.J. Chen, W. Rodi, A mathematical model for stratified turbulent flows and its application to buoyant jets, in: Proceedings of 16th Congress IAHR, Sao Paulo, Brazil, 1975.
[7] C.J. Chen, C.H. Chen, On prediction and unified correlation for decay of vertical buoyant jet, J. Heat Transfer 101 (1979) 532–537.
[8] M.R. Malin, The prediction of vertical, turbulent plume by use of the k–ϵ and k–w models of turbulence, Technical Report No. 9, Department of Mechanical Engineering, Imperial College of Science and Technology, London, UK, 1983.
[9] J.F. Sini, I. Dekeyser, Numerical prediction of turbulent plane jets and force plumes by use of the k–ϵ model of turbulence, Int. J. Heat Mass Transfer 30 (9) (1987) 1787–1801.
[10] D.J. Bergstrom, A.B. Strong, G.D. Stubley, Algebraic stress model prediction of a plane vertical plume, Numer. Heat Transf., A 18 (1990) 263–281.
[11] A. Pantokratoras, Effect of ambient temperature on vertical turbulent buoyant water jets, Int. J. Heat Mass Transfer 44 (2001) 1889–1898.
[12] M.R. Malin, B.A. Younis, Calculation of turbulent buoyant plumes with a Reynolds stress and heat flux transport closure, Int. J. Heat Mass Transfer 33 (10) (1990) 2247–2264.
[13] K. Kalita, A. Dewan, A.K. Dass, Computation of the turbulent plane plume using the k–ϵ–$\overline{t'^2}$–γ model, Appl. Math. Model. 24 (2000) 815–826.
[14] B.R. Ramaprian, M.S. Chandrasekhara, Study of vertical plane turbulent jets and plume, Technical Report IIHR Report No 257, The Institute of Hydraulic Research, University of Iowa, Iowa City, IA, 1983.
[15] B.R. Ramaprian, M.S. Chandrasekhara, Measurements in vertical plane turbulent plumes, J. Fluids Eng. 111 (1989) 69–77.
[16] W. Rodi, Turbulence Models and Their Application in Hydraulics—A State of the Art Review, Int. Assoc. Hydr. Res., Delft, 1980.
[17] M.R. Malin, D.B. Spalding, The prediction of turbulent jets and plumes by use of k–w model of turbulence, PCH, Physicochem. Hydrodyn. 5 (2) (1984) 153–198.

[18] A. Dewan, J.H. Arakeri, J. Srinivasan, A new turbulence model for the axisymmetric plume, Appl. Math. Model. 21 (1997) 709–719.
[19] S.V. Patankar, Numerical Heat Transfer and Fluid Flow, Hemisphere Publishing Corporation, New York, 1980.
[20] J.R. Cho, M.K. Chung, A k–ϵ–γ equation model, J. Fluid Mech. 237 (1992) 301–322.
[21] C.J. Chen, W. Rodi, Vertical Turbulent Buoyant Jets—Review of Experimental Data, Technical Report, vol. 4, Pergamon Press, Oxford, 1980.
[22] E.J. List, Turbulent jets and plumes, Ann. Rev. Fluid Mech. 114 (1982) 264–271 (Technical report).
[23] B.R. Ramaprian, M.S. Chandrasekhara, Intermittency and length scale distributions in a plane turbulent plume, J. Fluids Eng. 112 (1990) 367–369.